Genome-Wide Copy Number Analysis in Esophageal Adenocarcinoma Using High-Density Single-Nucleotide Polymorphism Arrays

Derek J. Nancarrow,[1] Herlina Y. Handoko,[1] B. Mark Smithers,[3] David C. Gotley,[3] Paul A. Drew,[5,6] David I. Watson,[7] Andrew D. Clouston,[4] Nicholas K. Hayward,[1] and David C. Whiteman[2] for the Australian Cancer Study and the Study of Digestive Health

[1]Oncogenomics and [2]Cancer and Population Studies, Queensland Institute of Medical Research, Herston, Queensland, Australia; [3]Upper Gastrointestinal and Soft Tissue Unit, Princess Alexandra Hospital, and Department of Surgery, University of Queensland, Princess Alexandra Hospital; [4]School of Medicine, Southern Clinical Division, Princess Alexandra Hospital, Woolloongabba, Queensland, Australia; [5]Department of Surgery, University of Adelaide, Royal Adelaide Hospital, Adelaide, South Australia, Australia; and [6]School of Nursing and Midwifery and [7]Department of Surgery, Flinders University, Bedford Park, South Australia, Australia

Abstract

We applied whole-genome single-nucleotide polymorphism arrays to define a comprehensive genetic profile of 23 esophageal adenocarcinoma (EAC) primary tumor biopsies based on loss of heterozygosity (LOH) and DNA copy number changes. Alterations were common, averaging 97 (range, 23–208) per tumor. LOH and gains averaged 33 (range, 3–83) and 31 (range, 11–73) per tumor, respectively. Copy neutral LOH events averaged 27 (range, 7–57) per EAC. We noted 126 homozygous deletions (HD) across the EAC panel (range, 0–11 in individual tumors). Frequent HDs within *FHIT* (17 of 23), *WWOX* (8 of 23), and *DMD* (6 of 23) suggest a role for common fragile sites or genomic instability in EAC etiology. HDs were also noted for known tumor suppressor genes (TSG), including *CDKN2A, CDKN2B, SMAD4*, and *GALR1*, and identified *PDE4D* and *MGC48628* as potentially novel TSGs. All tumors showed LOH for most of chromosome 17p, suggesting that TSGs other than *TP53* may be targeted. Frequent gains were noted around *MYC* (13 of 23), *BCL9* (12 of 23), *CTAGE1* (14 of 23), and *ZNF217* (12 of 23). Thus, we have confirmed previous reports indicating frequent changes to *FHIT, CDKN2A, TP53,* and *MYC* in EAC and identified additional genes of interest. Meta-analysis of previous genome-wide EAC studies together with the data presented here highlighted consistent regions of gain on 8q, 18q, and 20q and multiple LOH regions on 4q, 5q, 17p, and 18q, suggesting that more than one gene may be targeted on each of these chromosome arms. The focal gains and deletions documented here are a step toward identifying the key genes involved in EAC development. [Cancer Res 2008;68(11):4163–72]

Introduction

During the past 3 decades, there have been significant increases in the incidence of esophageal adenocarcinoma (EAC). In the United States, rates have risen faster than any other cancer (1–3), with similar increases documented in Europe (4, 5) and Australia (6, 7). With the increasing prevalence of contributing factors (i.e., obesity and acid reflux; ref. 8) in developed societies, it is predicted that EAC incidence will continue to rise, posing an escalating health burden. Better understanding of the genes involved, combined with increased knowledge of risk factors, may lead to improved screening and treatment. Although candidate screening approaches have implicated a few genes related to EAC development (reviewed in ref. 9), few studies have conducted detailed analyses on a genome-wide scale.

DNA copy number changes frequently contribute to tumor progression. Loss of tumor suppressor genes (TSGs), such as *CDKN2A* and *TP53*, commonly occurs in cancerous and precancerous conditions, including those of the esophagus (reviewed in ref. 10). In other genomic regions, copy number gain leads to the increased activity of oncogenes (e.g., *MYC*), which promote autonomous cell growth. Numerous TSGs and oncogenes have been shown to have a wide range of cellular functions and cancer specificities. There is little doubt that additional genes with roles in tumorigenesis await identification and whole-genome methodologies offer a powerful means to identify such genes.

Several studies have applied low-resolution comparative genomic hybridization (CGH) methodologies to investigate DNA copy number alterations in EAC (11–13). This technology adequately detects high-level amplifications and homozygous deletions (HDs) but underestimates loss of heterozygosity (LOH; ref. 14). The application of high-density single-nucleotide polymorphism (SNP) microarrays to define genome-wide copy number changes provides superior resolution and combines the advantages of both CGH and LOH methodologies, allowing the detection of copy neutral LOH (NLOH) events (15, 16). Here, SNP arrays were used to generate high-resolution DNA copy number profiles in a panel of primary EAC tumor biopsies.

Materials and Methods

Biopsy collection and DNA extraction. Approval to undertake the study was obtained from the research ethics committees of the Queensland Institute of Medical Research and participating hospitals. Written informed consent to participate was obtained from all patients. Primary EAC biopsies were taken from 26 patients (25 male and 1 female) before treatment. A biopsy of normal squamous esophageal epithelium from one patient was used as a reference sample. Biopsies were placed in RNAlater (Ambion) immediately on collection and left at 4°C overnight. Samples were then stored at −20°C before removal of excess RNAlater before storage at −70°C. DNA and RNA were simultaneously extracted using Qiagen AllPrep extraction kits via the Tissue Lyser–based protocol according

Note: Supplementary data for this article are available at Cancer Research Online (http://cancerres.aacrjournals.org/).

Requests for reprints: Derek J. Nancarrow, Oncogenomics, Queensland Institute of Medical Research, 300 Herston Road, Herston, Queensland 4029, Australia. Phone: 61-7-33620323; Fax: 61-7-38453508; E-mail: derek.nancarrow@qimr.edu.au.

doi:10.1158/0008-5472.CAN-07-6710

Table 1. Demographic details for 26 EAC biopsy patients

Patient no.	Sex	Age at diagnosis	Survival (d)	Status	Postoperative stage	Diagnosis*	Tumor % by LOH only †
40357	M	66	466	Alive	III	Slide review	28
53111	M	66	70	Alive	Not staged	Pathology report	30
40327	M	70	666	Alive	III	Pathology report	30
40323	M	60	531	Dead	IVA	Slide review	51
40353	M	63	536	Alive	III	Slide review	54
40359	M	55	469	Alive	I	Slide review	58
40358	M	56	408	Dead	IVA	Slide review	58
40340	M	66	329	Dead	IV	Slide review	59
40362	M	65	183	Dead	IVA	Slide review	61
54043	M	73	1,130	Alive	II	Pathology report	63
40331	M	65	600	Alive with disease	III	Pathology report	63
42199	F	74	634	Alive	IIA	Pathology report	65
40361	M	75	282	Dead	III	Slide review	67
54014	M	80	367	Dead	Not staged	Pathology report	67
53048	M	70	1,153	Alive	II	Pathology report	67
40356	M	78	489	Dead	III	Slide review	69
40341	M	79	391	Dead	III	Slide review	78
40363	M	69	462	Alive	I	Pathology report	78
40334	M	68	607	Alive	IIA	Slide review	78
40325	M	62	657	Dead	IIA	Slide review	84
40338	M	72	53	Dead	IVB	Slide review	85
40320	M	62	699	Alive	IIB	Slide review	87
53145	M	52	878	Alive	IV	Pathology report	88
40360	M	78	452	Alive	IIA	Slide review	89
40364	M	71	287	Dead	IVA	Slide review	90
40345	M	61	547	Dead	III	Slide review	91

* EAC diagnosis was confirmed by review of a H&E slide made from a tumor biopsy from the same esophageal level as the DNA sample biopsy (slide review). Where this was not possible, diagnosis was confirmed through review of the existing pathology report. In all cases, the review was conducted by the same experienced pathologist (A.D.C.).

† Determined from the Ballele fraction in designated LOH regions using SiDCoN (18).

to the manufacturer's instructions (Qiagen). Diagnosis was confirmed by pathologic review (by A.D.C.) of a separate biopsy taken from the same lesion (n = 17, usually at the same level of the esophagus) or by clinical review (n = 9). Patient information was collected through self-completed, mailed questionnaires and clinical chart review (8); salient features are summarized in Table 1.

SNP microarray preparations. The Infinium II Assay was done using Illumina Sentrix HumanHap300 BeadChips (317K, TagSNP Phase I, v1.1) according to the manufacturer's specifications (Illumina). Briefly, 750 ng of genomic DNA were amplified at 37°C overnight using solutions WG-AMM and WG-MP1, following which the amplified DNA was fragmented using solution WG-FRG and precipitated with isopropanol after the addition of WG-PA1. Dried pellets were then resuspended in WG-RA1 and hybridized to beadchips along with WG-RA1 and formamide. Arrays were incubated overnight at 48°C, after which they underwent single-base extension on a TeFlow Chamber Rack system (Tecan) using solutions WG-XC1, WG-XC2, and WG-TEM. Following which, they were stained with WG-LTM and WG-ATM, dried for 1 h, and then imaged using a BeadArray Reader (Illumina). Image data were analyzed using BeadStudio 2.0 (Illumina). For additional details and example outputs, refer to Peiffer and colleagues (17). All genomic positions were based on hg17 from the University of California at Santa Cruz (UCSC) Genome Browser.[8]

Compilation of individual EAC profiles. BeadStudio 2.0 software was used to generate whole-genome profiles for the tumors. Each EAC was referenced against a sample of normal squamous epithelium. As noted previously (17), this approach provided more consistent logR ratios compared with using the common reference pool provided by Illumina. We compared this squamous sample against the Illumina reference pool and found it to have a normal 2n DNA complement, with the exception of a very small region of amplification within chromosomal band 6q27. Thus, SNPs mapping within the 6q27 chromosomal band were excluded from analysis. Because the HumanHap300 Genotyping BeadChip only includes two SNPs that map to the Y chromosome, we also excluded this chromosome from our analyses. The process EAC and squamous reference data files are in the Gene Expression Omnibus, series GSE10506.

Initially, we used the autoscoring procedures built into BeadStudio 2.0 (LOH score and copy number variation algorithms); however, these yielded inconsistent output in the presence of nontumor tissue contamination. Thus, all DNA copy number regions were annotated manually by one of us (D.J.N.) and confirmed by another (H.Y.H.) with the aid of our Simulated DNA Copy Number (SiDCoN) tool (18). Any discrepancies between scorers were discussed and consensus was reached. With the exception of HD and 4n gain events (which both have normal Ballele profiles but grossly altered logR values), we did not score DNA changes if Ballele plots indicated that <30% of cells were involved, as described previously (18). DNA copy number changes for all samples were converted using Excel into custom data tracks for the UCSC Genome Browser.

Estimations of tumor cell density in biopsy samples. Tumor biopsies contain a variable amount of normal tissue. High levels of nontumor tissue

[8] http://genome.ucsc.edu/

interfere with DNA copy number interpretations of tumor samples. We thus estimated the tumor fraction of each biopsy using the following procedure: regions of LOH were identified manually; the level of Ballele involvement was determined within each of these regions by exporting the Ballele data for each sample from BeadStudio; using an R script, Ballele values <0.5 were inverted, providing plots ranging from 0.5 to 1 (this step essentially doubles the density of the Ballele signal intensity measures, providing more accurate estimates, particularly for shorter DNA copy number changes); and a smoothed binary segregation algorithm (19) was then applied, across each chromosome, to the modified Ballele values <0.97 (polymorphic SNPs), generating regionally normalized data for each SNP. Another R script was then used to identify the SNPs that mapped within each LOH event and average the normalized Ballele values within the appropriate tumor sample. Using SiDCoN (18), we then estimated the tumor involvement within each of these events. Across each sample, the LOH events with the highest tumor involvement were assumed to approximate the total fraction of tumor in each sample. This procedure assumes that contaminating nontumor tissue has a normal 2n DNA complement. The result of this analysis (presented in Table 1) showed that 3 of our 26 EAC biopsies contained <50% tumor material. These samples were excluded from further study because the Illumina platform has been found insensitive when tumor content drops below this level (17). The remaining 23 EAC biopsies contained 50% to 90% tumor cells based on the strongest LOH changes.

Median logR plots. Sample-specific logR data were exported from BeadStudio 2.0 for the 23 EAC biopsies with >50% tumor cells, as described above. R scripts were used to apply a smoothed binary segregation algorithm (19) to these data for each sample across each chromosome. These data were then compiled to generate median (smoothed) logR values across each data point.

Results

Sample details. Average age at diagnosis was 67 years (range, 52–80). The cohort included two stage I, seven stage II, eight stage III, and seven stage IV patients based on postoperative staging, with patient survival times ranging from 53 to 699 days and a minimum follow-up time of 70 days for surviving patients. Consistent with the previous genome-wide array studies (11–13),

Table 2. Key regions of DNA copy number change in 23 EAC biopsies

Region in hg17	Size (Mb)	Chromosomal band	DNA alterations	Possible genes of note
A. Regions of fewest changes				
chr1:1,300,001-7,300,000	6.0	1p36.32	9 changes	p36.3 breakpoint, *TP73, DFFB*
chr10:76,700,001-81,900,000	5.2	10q23.3	9 changes	
chr11:102,400,001-115,000,000	12.6	11q22.3-q23.1	10 changes	Includes *CASP4, CASP5, CASP1*, and *ATM* gene
chr16:6,300,001-11,300,000	5.0	16p13.2	10 changes	
B. Most common gain (AMP) regions (smallest region or overlap is indicated)				
chr18:18,180,001-18,280,000	0.1	18q11.2	14 AMPs	*CTAGE1*
chr8:101,100,001-104,000,000	2.9	8q22.3	13 AMPs	*MYBL1*
chr8:128,100,001-129,100,000	1.0	8q24.21	13 AMPs	*MYC*
chr8:130,500,001-132,000,000	1.5	8q24.21	13 AMPs	*MLZE, DDEF1*
chr1:143,700,001-144,900,000	1.2	1q21.1	12 AMPs	*BCL9*
chr1:151,000,001-155,000,000	4.0	1q22	12 AMPs	*SKI*
chr20:49,100,001-52,300,000	3.2	20q13.2	12 AMPs	*ZNF217*
C. Most common LOH regions (smallest region or overlap is indicated)				
chr18:42,300,001-49,000,000	6.7	18q21.1	18 LOHs (HD region)	
chr18:54,600,001-58,000,000	3.4	18q21.32	18 LOHs (HD region)	*MC4R*
chr17:1-20,774,742	20.8	17p	16-15 LOHs	Many including *TP53, MYBBP1A*
chr5:55,000,000-93,500,000	38.5	5q11.2-q14.3	14 LOHs (HD region)	Many including *PDE4D*
chr11:2,400,000-5,900,000	3.5	11p15.4	14 LOHs	Many including *CDKN1C*
D. Most common regions of shared copy NLOH (smallest region or overlap is indicated)				
chr2:10,000,000-85,000,000	75.0	2p24.3-p12	11 NLOHs	Many including *MSH2, MYCN*
chr2:230,000,001-238,400,000	8.4	2q37	10 NLOHs	Many
chr9:134,500,001-137,500,000	3.0	9q34.3	10 NLOHs	Many including *TSC1*
chr17:6,800,000-7,700,000	0.9	17p13.1	10 NLOHs	Many including *TP53*
chr17:400,000-1,400,000	1.0	17p13.3	10 NLOHs	Many
chr17:74,800,000-77,000,000	2.2	17q25.3	10 NLOHs	Many
E. Most common regions of HD (smallest region or overlap is indicated)				
chr3:60,310,078-60,712,164	0.4	3p14.2	17 HDs	Within *FHIT*
chr16:76,691,052-77,804,064	1.1	16q23.2	8 HDs	Within *WWOX*
chr9:21,580,000-22,600,000	1.0	9p21.3	6 HDs	Includes *MTAP, CDKN2A, CDKN2B, C9orf53, DMRTA1*
chrX:30,898,403-32,989,184	2.1	Xp21.2	6 HDs	Within *DMD*
chr4:91,513,360-92,060,333	0.5	4q22.1	5 HDs	Within *MGC48628*
chr18:46,700,000-46,950,000	0.3	18q21.1	4 HDs	Includes *ME2, ELAC1, SMAD4*
chr18:72,900,000-73,900,000	1.0	18q23	4 HDs	Includes *MBP, GALR1*
chr5:58,306,241-59,819,647	1.5	5q11.2-q12.1	3 HDs	Within *PDE4D*
chr18:56,050,001-56,400,000	0.3	18q21.32	3 HDs	Includes *MC4R*
chr9:24,300,000-25,800,000	1.5	9p21.3-p21.2	2 HDs	No genes
chr20:14,500,000-15,536,000	1.0	20p21.1	2 HDs	Includes *20orf133, BBC018687*
chr21:21,500,001-25,000,000	3.5	21q21.1-q21.2	2 HDs	Includes *NCAM2, FLJ42200*

Figure 1. A region of chromosome 3p14.2 centered on the *FHIT* gene, viewed in the UCSC browser, May 2004 (hg17) build of the human genome. The custom tracks represent profiles for 23 EAC biopsies with DNA copy number status noted by the shades: *no fill,* gain; *light gray,* NLOH; *gray,* LOH; *black,* HD.

and most EAC publications, our cohort has a strong male bias. As expected, the postoperative staging correlates significantly with patient survival [P = 0.0136, Cox proportional hazards (CPH)], whereas age (P = 0.1336, CPH) and the nontumor content of the biopsy (P = 0.2304, CPH) do not.

Types and numbers of DNA copy number changes. We observed 2,229 DNA copy number changes across all 23 EAC samples, an average of 97 per tumor (range, 23–208; Supplementary Table S1). Within these changes, 20% to 90% of the genome showed a change in DNA copy number in each EAC biopsy. This suggests a high background rate, with at least 39% (9 of 23) of our EAC primary tumor panel showing DNA copy number changes at any autosomal point. The genomic regions with the least number of changes were 1p36.32 and 10q23.3 with 9 changes and 11q22.3 and 16p13.2 with 10 changes (Table 2A). In each case, the type of changes seen was a roughly even mix of losses, NLOH, and gains, with the exception of 11q22.3, which was mostly LOH (8 of 10).

The most common changes were LOH and gains, with averages of 33 (range, 3–83) and 31 (range, 11–73) per EAC, respectively (Supplementary Table S1). SNP arrays allow the detection of copy NLOH (15, 16), which was surprisingly common, averaging 27 (range, 7–57) per EAC. LOH and NLOH changes tended to be larger, averaging 18 and 23 Mb, respectively, compared with 13 Mb for gains (Supplementary Table S1). Within each sample, LOH and NLOH changes were seen in an average of 20% of the genome, but the range within individual EACs was very large (3–52%). These changes often spanned a whole chromosome arm. It is noteworthy that in some biopsies the majority of LOH changes tended to involve all tumor cells, whereas others exhibited variable proportions of tumor cell involvement. Examining the tumor panel based on this variable revealed that it was variable, rather than categorical, with most samples exhibiting some to many LOH regions with <100% tumor cell involvement.

We noted 126 HDs within the EAC panel, ranging from 0 to 11 in individual tumors (Supplementary Table S1). Of these, 29 (23%) were partial HDs such that some DNA remained within a proportion of tumor cells. This was determined manually using SiDCoN (18) to show that the observed logR and Ballele pattern resulted from mixed cell populations. Partial HDs generally arose within a LOH or NLOH event, which perhaps demarks the initial allelic loss. When the mixed populations included a combination of HD, LOH, and normal cells or HD, NLOH, and normal cells, both

Ballele and logR changes were used to determine the presence of the HD. In some samples, partial HD events spanned up to 100 Mb; however, HD regions in general were much smaller (<10 Mb) than the other DNA copy number changes observed.

Considering the different DNA copy number changes outlined above, the number of each type of change or the fraction of the genome involved does not seem to relate to patient survival (all CPH tests yielded $P > 0.1$) or tumor stage ($P > 0.1$, ANOVA).

Key regions of gain. It is worth noting that NLOH changes can be considered, along with LOH, as the loss of a functional allele (then duplication of the null/reduced allele) or with gains as a duplication of an overactive oncogenic allele (and removal of the normal allele). In this way, it is important to note NLOH changes within regions of either high LOH or gain. Table 2B shows those chromosomal regions with the most number of EAC biopsies showing concomitant gain. The indicated regions represent the smallest hg17 location shared among all amplified samples. It is interesting that the region with the highest number of gains is within 18q11.2, on a chromosome arm well documented as lost in EAC. This is also the region in which we saw the most amplifications, with 4 of the 14 gained samples showing greater than five copies within 18q11.2. Although we also observed loss further down the chromosome arm, this region of shared gain was present in >60% of our samples and a further four EACs (17%) had NLOH. The only known gene within the minimal region of overlap between the 14 amplified samples (Table 2B) is *CTAGE1*, which is expressed in a variety of cancer types (20).

Chromosome 8 contained three key regions of gain (8q22.3-8q24.21), each involving the same 13 (56%) biopsies. The individual regions range in size from 1 to 3 Mb (Table 2B). The two smaller regions, both in 8q24.21, seem to specifically target known oncogenes (*MYC, MLZE*, and *DDEF1*), whereas the larger region (8q22.3) contains several genes, including *MYBL1*.

The EAC panel showed frequent gains on chromosome 20, most commonly a 2.9-Mb section of 20q13.2. One sample, 40334, was amplified spanning chr20:49397548-50700650, whereas 53048 showed a 4n gain at chr20:50788541-51029249 and strong (9n) gain between chr20:51029250-52711041. The latter region contains several genes, including the oncogene *ZNF217*.

We observed two regions on the long arm of chromosome 1 with gains in >50% of EACs: chr1:143,700,001-144,900,000, centered on *BCL9* in 1q21.1, and chr1:151,700,000-152,300,000 in 1q22 (Table 2B). The latter region, defined by a 3n gain in 40334, contains many genes, including *MUC1*, which is known to have oncogenic potential (21) and to be frequently overexpressed in EACs (22).

Key regions of loss. We identified two types of LOH events within our data, regions that include frequent HD events, such as *FHIT* (Fig. 1), and areas of LOH with no accompanying HDs, such as 17p (Supplementary Fig. S1), suggesting potentially different mechanisms of action. Regions where two or more EAC biopsies had overlapping HDs are shown in Table 3. All known genes that map within each of these regions are listed. In several cases, for example, *FHIT* (3p14.2), *WWOX* (16q23.2), *DMD* (Xp21.2), *MGC48628* (4q22.1), and *PDE4D* (5q11.2-q12.1), the smallest region of overlap between the contributing samples can be narrowed to within a gene. The smallest region of overlap within *FHIT* is a 20- to 25-kb region within intron 4, defined by 17 HD events (Fig. 1).

On chromosome 9p, six samples had HDs (Table 2E), which overlapped such that the smallest region includes five genes: *MTAP, CDKN2A, CDKN2B, C9orf53*, and *DMRTA1* (Supplementary Fig. S2). Both *CDKN2A* and *CDKN2B* are recognized TSGs, and several reports have noted *CDKN2A* deletions and mutations in EAC (reviewed in refs. 9, 10). In our cohort, most HD events on chromosome 9 clustered on 9p21.3, although 42199 has two separate HD events [9p21.3 (chr9:20009316-22549868) and 9p21.2-9p21.1 (chr9:27354350-30507289)] and a single HD in 40334 spans 9p21.1-pter (Supplementary Fig. S2).

We found three regions with HDs, 18q21.1, 18q21.32, and 18q23, which center on a total of six genes (Table 3), two of which (*SMAD4* and *GALR1*) are TSGs. Two EACs (40356 and 40364) had separate HD events across 18q and two HD events span more than half the telomeric end of these arms, further supporting the hypothesis that there are multiple TSGs in this region.

Our analysis specifically identified *MGC48628* (4q21.1) as a potential TSG, with three (40345, 40358, and 42199) of five HDs mapping within, or exclusively including, this gene. Six other samples had LOH across *MGC48628*, two more switched from NLOH to LOH within it, whereas another EAC was NLOH across the gene.

Table 2C presents a broad region of frequent LOH on chromosome 5q (5q11.2-q14.3), whereas Table 2E shows three HDs that focus on *PDE4D* (at the border or 5q11.2-q12.1). In the latter region, 15 of 23 EACs had either LOH or HD, and two others showed NLOH. By comparison, 10 samples had LOH for *APC,* whereas 4 had NLOH for all, or part, of the gene.

Table 3 lists all HDs seen in two or more samples, and the samples in which they occurred. None of the regions with two or more HD samples (Table 3), nor all of them combined, provided any evidence of association with patient survival (CPH) or tumor stage (*t* test; data not shown).

Several regions contained high level of DNA loss but few HDs. The most prominent of these was on chromosome 17p, where all 23 EACs showed LOH (Table 2C) or NLOH (Table 2D) changes for most of the short arm, spanning chromosomal bands 17p12-p13.2 (Supplementary Fig. S1). Historically, *TP53* (17p13.1) is frequently lost or mutated in EAC (10). Our data did not specifically implicate *TP53*; in fact, the broad overlapping region of change shown in Supplementary Fig. S1 suggested additional targets on 17p. Furthermore, the single HD event present on 17p did not include *TP53*. Given that several samples shifted back and forth between LOH and NLOH, it is difficult to ascertain a more defined target region. If we assume NLOH to be more important, then the regions 442766-1386639 (which includes *ABR* and *TUSC5*) and 6879962-7662915 (which includes *BCL6B, TP53*, and *POLR2A*) both contained 10 NLOH events and 13 LOH events across the 23 EAC biopsies, whereas if we assume LOH to be more important the region chr17:12378912-15024426 (17p12), defined by sample 41299, included 16 LOH and 7 NLOH events. The only HD detected on chromosome 17p (10868740-11363397) targeted *FLJ45455* and there were 15 LOH and 7 NLOH events across the same region.

Within chromosomal band 11p15.4, there were two small adjacent regions (283572-10868740 and 10868740-21670355) with 14 LOH, 3 NLOH, and no HD and 15 LOH, 2 NLOH, and no HD events, respectively.

Averaged gain/loss plots. Figure 2 shows median logR values across each chromosome. The black line shows the median values, whereas the gray margins demark the 75% (upper quartile) and 25% (lower quartile) levels across all 23 samples. This format allows for more direct comparison of our results to those of the previous CGH

Table 3. Regions with 2 or more HDs within 23 EAC biopsies

Minimal HD regions	Chromosomal band	No. HDs	40320	40323	40325	40331	40334	40338	40340	40341	40345	40353	40356	40358	40359	40360	40361	40362	40363	40364	42199	53048	53145	54014	54043
chr3:60,310,078-60,712,164	3p14.2	17	×			×	×	×	×		×		×		×	×	×	×	×	×		×	×	×	×
chr16:76,691,052-77,804,064	16q23.2	8	×		×	×			×	×						×		×	×						
chr9:21,580,000-22,600,000	9p21.3	6	×				×				×			×					×		×				
chrX:30,898,403-32,989,184	Xp21.2	6				×				×					×	×		×							×
chr4:91,513,360-92,060,333	4q22.1	5			×						×			×						×	×				
chr18:46,700,000-46,950,000	18q21.1	4											×						×	×			×		
chr18:72,900,000-73,900,000	18q23	4											×							×	×		×		
chr5:58,306,241-59,819,647	5q11.2-q12.1	3	×					×								×									
chr18:56,050,001-56,400,000	18q21.32	3						×												×			×		
chr9:24,300,000-25,800,000	9p21.3-p21.2	2					×					×													
chr20:14,500,000-15,536,000	20p21.1	2			×														×						
chr21:21,500,001-25,000,000	21q21.1-q21.2	2					×															×			

and LOH studies because NLOH events were not highlighted. Using a median gain of >0.2 as a cutoff (with a value of 0.33 indicating all cells show a 3n complement for that DNA fragment), we found gains on 1q, 2q, 7p, 8q, 12p, 13q, 18q, 20p, and 20q. Peak median gains (>0.27) occurred at 8q23.3 (chr8:113800000-113900000) within the *CSMD3* gene, where 11 samples were amplified, and on 13q12.13 (chr13:24660000-24680000) near *FLJ25477*, where 8 samples were amplified.

The sharply defined losses on chromosomes 3p and 9p, with median logR values of less than −0.35 (Fig. 2), corresponded to HDs within *FHIT* and 9p21.3 (containing *CDKN2A* and *CDKN2B*; Fig. 1; Supplementary Fig. S2). The region surrounding *WWOX* on 16q was evident from the combined data (Fig. 2) but not to the same extent due to the large number of NLOH events rather than the relatively high number of LOH changes seen on 9p. Other extended regions of loss, with median values of less than −0.2, mapped to 4p, 4q, 5q, 11p, 16p, 17p, 18q, 19p, and 22q (Fig. 2).

By using >0.3 for the 75% quartile level and less than −0.3 for the 25% level, we have flagged regions altered in a minority (~25%) of samples. This added gains on 3q and 5p and deletions of 16q, 21q, and Xp. Table 4 summarizes these data across all chromosome arms, incorporating evidence drawn from previous CGH and LOH genome-wide DNA copy number studies done on EACs, which is discussed in detail below.

Discussion

Previous studies reported a high background rate of DNA copy number change (20–30%) in EAC. We found a similar rate (40%) when one considers that about one third of the changes we observed are NLOH events, not detected by previous CGH studies. In Table 4, the highlighted regions summarized for each study indicate either gain (AMP), loss (LOH), or allelic imbalance (AI) in Gleeson and colleagues (23), who did not distinguish loss and gain events. Given this high background rate, it is not surprising that only 10p and 18p (along with most acrocentric arms) show no highlighted regions in any of the 10 studies (Table 4). Adopting a pragmatic approach, we believe further investigation is required into all chromosomal regions where three studies or less have reported frequent changes. Important EAC genes may lie within

these regions; however, a much larger sample size would be required to clarify whether genes within these regions play a significant role in EAC etiology.

Given the strength of the 3p14 findings from our cohort (>70% HD within *FHIT*) and others (24), it is surprising that only three of the other nine studies in Table 4 report noteworthy LOH on chromosome 3p. A partial explanation may lie in the fact that, of the 22 samples in our study that showed loss on 3p, only 8 show extensive regions of loss (Fig. 1); thus, low-density studies, such as that of Hammoud and colleagues (25) with only a single marker at 3p25, may have missed the peak region within *FHIT*. This does not explain the data of Weiss and colleagues (26), however, where concomitant CGH analysis of esophageal squamous cell carcinoma showed high levels of 3p deletion (64%), yet only 4% of their 24 EACs showed deletion on 3p.

Similar to *FHIT* (FRA3B), *WWOX* (FRA16B) and *DMD* (FRAXC) occur within common fragile sites. Our data also showed frequent HD within the latter two genes. We found NLOH events to be frequent on 16q, masking its potential significance in the median logR plot (Fig. 2), and in previous CGH studies that could not detect NLOH events. Furthermore, given the low resolution of microsatellite LOH studies listed in Table 4 (39–138 markers), it is also likely that other studies would have missed intragenic deletions within *WWOX*. Thus, it is unclear whether previous genome-wide studies did not detect losses in common fragile sites or whether these changes are only present in a subset of EACs. The group that previously reported HDs within *FHIT* (24) also observed changes in other fragile site genes *WWOX* (FRA16D) and genes within FRAXB (27). Because deletions targeting FRAXB have no known relevance to EAC tumor biology, Arlt and colleagues (27) propose that the increased activity of these fragile sites was a marker for genomic instability. Several lines of evidence link common fragile site stability to cell cycle checkpoints and DNA repair (reviewed in ref. 28). This does not negate the importance that loss of known TSGs *FHIT* and *WWOX* (reviewed in ref. 28, 29) could have on the progression of tumors with these changes; in fact, data indicate that these genes and the fragile sites they arise in are co-conserved (reviewed in ref. 29). Further work is required to characterize this phenomenon, to determine whether it is restricted to a subset of EAC patients, and to elicit specific roles for the disrupted genes.

The most consistent regions of frequent DNA loss in the literature are on 4q, 5q, 9p, 17p, and 18q, with particular foci on 4q22, 5q21, 9p21, 17p12, and 18q21-22 (Table 4; reviewed in ref. 9). On 4q, our cohort has highlighted *MGC48628* (4q21.1) with 56% LOH and three of five HDs involving only this gene. *MGC48628* maps within the minimal region of loss identified by Rumpel and colleagues (30) in 29 primary EAC tumors. Six other genome-wide studies (Table 4) support frequent 4q LOH; however, within these, there are two regions of loss: 4q22-23 (12, 13, 31) and 4p34-35 (11, 23, 25). Sterian and colleagues (32) reported frequent LOH on 4q, focused on 4q31-35. Taken together, these data suggest multiple target genes on this arm. Our median sample data (Fig. 2) showed a sharp trough at 4p22 (*MGC48628*) and a much broader region of loss at the telomere of 4q (4q34-35).

Chromosome 5q also shows frequent losses in 70% of studies (Table 4). The most common region of loss maps to 5q21, likely targeting *APC* (11–13). These data are supported by several microsatellite-based studies, which report >30% LOH in the vicinity

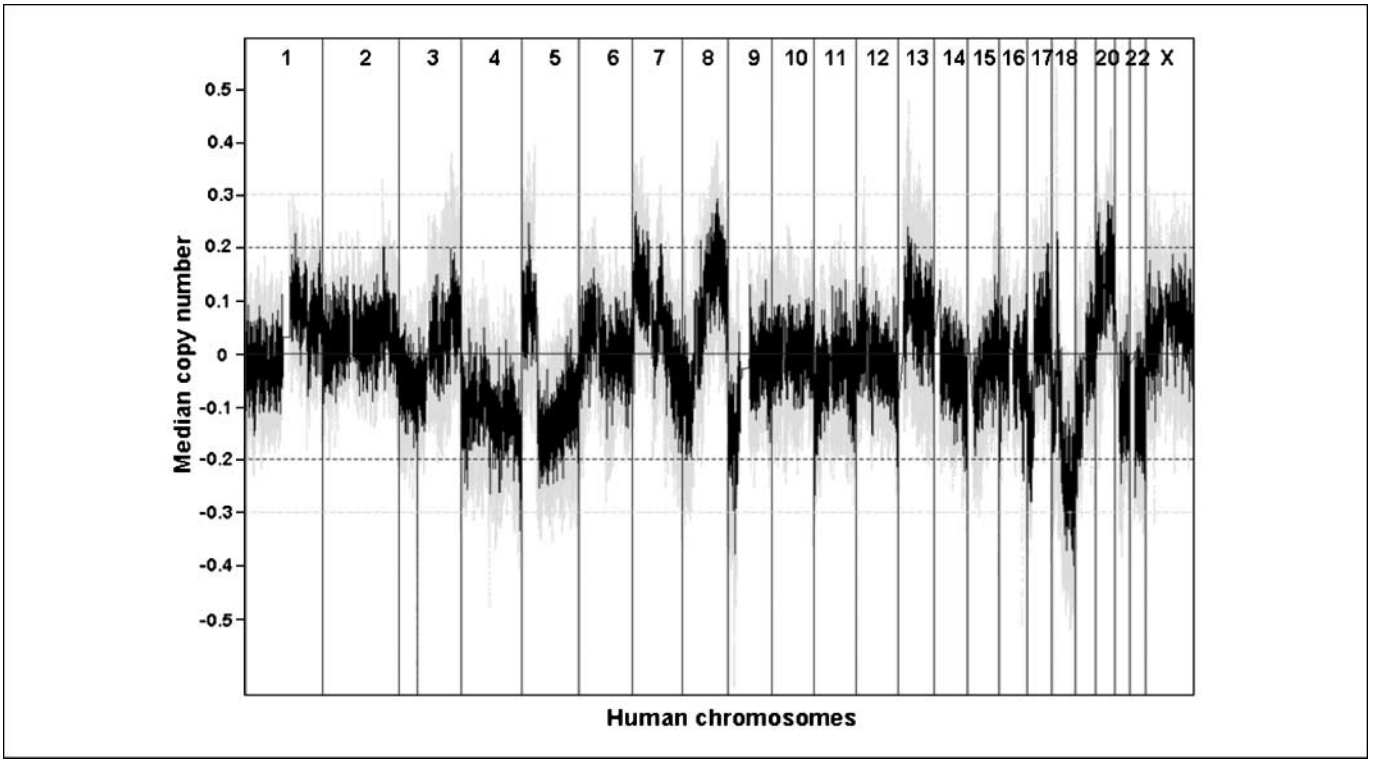

Figure 2. Median EAC biopsy logR values for chromosomes 1 to 22 and X. To generate this plot, the smoothseg algorithm (19) was applied to individual sample data and median values (*black*), across 23 EACs, were plotted in R. *Top* and *bottom light lines,* quartile values for each median value. Guide lines at 0.2 and −0.2 represent median value thresholds discussed in text, whereas light guides at 0.3 and −0.3 represent quartile thresholds.

Table 4. DNA copy number loss and gain summary of 10 genome-wide EAC tumor studies

Reference	Current study	van Dekken (12)	Riegman (11)	Walch (13)	Albrecht (36)	Barrett (44)	Gleeson (23)	Hammoud (25)	Varis (31)	Weiss (26)	Notes
Study type	SNP-aCGH	CGH	CGH	CGH	aCGH (287 genes)	43 MSATs	138 MSATs	39 MSATs	CGH	CGH	
No. EAC	23	28	30	30	18	20 (flow sorted)	17	27	18	24	
1p					AMP	LOH					
1q	AMP				LOH						
2p				AMP	AMP						~2p22.3
2q	AMP									AMP	2q33
3p	LOH	LOH	LOH		LOH						3p14.3
3q	AMP		AMP		AMP		AI			AMP	3q26
4p	LOH		LOH		AMP						Broad 4p
4q	LOH	LOH	LOH	LOH			AI	LOH	LOH		Broad 4q
5p	AMP	AMP			AMP						
5q	LOH	LOH	LOH	LOH		LOH	AI		LOH		5q11.2-q12.1, 5q21
6p		AMP		AMP							Broad 6p
6q							AI				
7p	AMP	AMP	AMP						AMP	AMP	~7p12, ~p15
7q			AMP/LOH	AMP	AMP					AMP	7q21
8p			LOH								8p21
8q	AMP	AMP	AMP	AMP	AMP				AMP	AMP	8q24.1
9p	LOH	LOH	LOH	LOH	AMP/LOH	LOH	AI				9p21
9q							AI		AMP		
10p											
10q				AMP					AMP		10q25-26
11p	LOH										11p15.5
11q					AMP						11q22.3
12p	AMP						AI				12p13.1
12q		AMP					AI				12q21.1
13p											
13q	AMP		LOH			LOH			AMP	AMP	13q12 (AMP), 13q14-31 (LOH)
14p											
14q		LOH	LOH	LOH							14q31-32
15p											
15q		AMP	AMP	AMP	AMP						15q25
16p	LOH										16p13.3
16q	LOH	LOH	LOH								16q23
17p	LOH	LOH	LOH		LOH	LOH	AI	LOH		LOH	17p12
17q		AMP	AMP	AMP/LOH	AMP				AMP		17p11, 17q21
18p											
18q	AMP/LOH	LOH		LOH	AMP	LOH	AI	LOH		LOH	18q11.2 (AMP), 18q21-q23 (LOH)
19p	LOH										
19q		AMP									
20p	AMP	AMP									20p12
20q	AMP	AMP	AMP	AMP					AMP	AMP	20q13.2-13.31
21p											
21q	LOH	LOH									21q21
22p					LOH						
22q	LOH		LOH								22q13.32
Xp	LOH										
Xq		AMP									23p21.1
Y	ND	LOH	LOH	LOH	ND	ND	ND	ND	ND	ND	

of *APC* (33, 34). In contrast, our EAC cohort shows LOH across much of 5q, with particularly strong regions of loss at 5q11.2-q12.1 and 5q14.3-31.1 (Fig. 2). The only three HDs observed on 5q are clearly centered on *PDE4D*, which borders on 5q11.2 and 5q12.1, supported by losses in 65% of our cohort compared with <45% in the vicinity of *APC*. Thus, *PDE4D*, rather than *APC*, seems to be the focus of 5q losses in our EAC cohort. HDs have recently been reported within *PDE4D* in lung adenocarcinoma (35), suggesting it is a putative TSG.

The broad LOH peak we observed on 18q (Fig. 2) is also present in six of the nine previous genome-wide reports in Table 4. Although the peak region seems to be within 18q21-22, containing the candidate TSGs *DCC, SMAD2*, and *SMAD4*, CGH studies report frequent loss of whole arm (11–13). Within our cohort, we have nine HDs on chromosome 18q, which tend to cluster at 18q21.1, 18q21.32, or 18q23, with several samples having multiple HD events across the arm implicating *SMAD4, GALR1*, and *MC4R*, whereas *DCC* and *SMAD2* fall outside critical HD events. We have identified a small (100 kb) region of gain at 18q11.2 (Fig. 2), suggesting the presence of both an oncogene as well as the one or more TSGs on this arm. The only gene that maps within this AMP is *CTAGE1*. An array CGH (aCGH) study noted that 39% (7 of 18) of their EACs were amplified for *LAMA3* (36), 1.3 Mb telomeric of *CTAGE1*. Further specific investigations will be needed to verify *CTAGE1* as a potential oncogenic target.

CDKN2A is one of the most frequently deleted genes across cancers, and it is most likely the target for LOH in 9p21, a frequent change noted in 7 of the 10 genome-wide studies in Table 4. Our data showed frequent (26%) HDs involving *CDKN2A*; however, the minimal region of overlap between the six HD events contained four other genes, including *CDKN2B*, another TSG. Several studies have shown losses, mutation, or hypermethylation of *CDKN2A* in EAC (10, 37–39).

All 23 of the EAC biopsies in this study showed DNA copy number variations along the length of the short arm of chromosome 17, generally LOH or NLOH. Changes to *TP53* (17p13.1) have been reported as frequent early events in EAC progression (40). However, others have noted that also multiple regions on 17p are the target of LOH events (41).

Three studies reported frequent Y chromosome loss in 40% to 76% of EACs (11–13). The underrepresentation of Y loss in Table 4 may be simply because so few studies have investigated it. Because the HapMap 330K SNP chips do not include Y-specific markers, we are unable to confirm this in our cohort. Given the strong male bias for this cancer, detailed investigation of the Y chromosome is warranted, especially because reintroducing Y has been shown to suppress the tumorigenic potential of other human cancer cells (42).

Table 4 shows that four to five genome-wide DNA copy number studies reported frequent gains on 3q, 7p, 7q, 15q, and 17q. Of these, our cohort has median logR peaks >0.2 on 3q and 7p. Looking across studies, focal points at 3q26, 7q21, and 15q25 can be determined. Although the regions on 7p are broad, 17q gains seem to center on 17q11 or 17q21 in different studies. Unlike the above listed regions, peak gains on 8q and 20q were very broad in our EAC panel (Fig. 2), suggesting the presence of multiple oncogenes and perhaps explaining why these were the most frequently amplified regions across the 10 studies (Table 4). Focal points of common gain across the studies can be narrowed to 8q24.1 and 20q13. The main target on 8q is believed to be *MYC*, although other surrounding oncogenes (including *MLZE, DDEF1*, and *MYBL1*) are frequently amplified. A novel amplicon resulting in the overexpression of *CTSB* has been shown in one study (43), indicating that this too may be a target for 8q gain. On chromosome 20q, candidate genes include *ZNF217* (36) and *MYBL2*, although the latter gene is not within our peak region.

In summary, we have generated the most comprehensive investigation of DNA copy number variation in EAC tumors to date. Our data indicate that structural genetic changes are very frequent events in EAC, with an average of 97 changes per tumor. These changes constitute roughly even proportions of gain, LOH, and NLOH events, which together spanned 20% to 90% of the individual tumor genomes. HDs were relatively infrequent, 0 to 11 per tumor, and tended to be highly focused. We confirm that deletion within *FHIT* is one of the most common events in EACs (24). Frequent HDs within *FHIT* (3p14.3), *WWOX* (16q), and *DMD* (Xp) suggest a role for common fragile sites in EAC etiology; alternatively, decreased genomic stability may be a critical marker for a subset of EAC tumors. Aside from *FHIT*, these regions seem to be infrequent sites of loss in other EAC DNA copy number studies. This may be an issue of technical sensitivity (detection density) or it may indicate an as yet unidentified EAC stratification. Our data also showed multiple HDs targeting *PDE4D* (5q11.2-q12.1) and possibly *SMAD4* (18q21.1) and *GALR1* (18q23), which appear in the chromosomal regions frequently lost in previous studies (Table 4). In addition, we found HDs clustered within the gene *MGC48628* (4q22.1), making it a potential novel TSG.

Meta-analysis of the 10 genome-wide CGH and LOH studies summarized in Table 4 indicates that the most common sites for gain in EAC are 8q24 and 20q13. The broad peaks generally observed in these regions suggest that multiple oncogenes are involved and our results are consistent with this. Additionally, we have identified a frequent, focused gain within 18q11.2, centered on *CTAGE1*. Across the 10 studies, regions on 4q, 5q, 9p, 17p, 18q, and Y are the most frequently lost in EAC. The target genes seem to include the TSGs *APC* (5q21), *CDKN2A* (9p21.3), and *TP53* (17p12), although other genes on 5q and 17p also seem to be critically lost. The key genes on 4q, 18q, and Y have yet to be identified. Comprehensive genomic profiling such as that presented here will allow a more defined approach to identifying and characterizing genes involved in EAC progression, offering the potential for improved clinical tests and treatments.

Disclosure of Potential Conflicts of Interest

No potential conflicts of interest were disclosed.

Acknowledgments

Received 12/19/2007; revised 2/15/2008; accepted 3/2/2008.

Grant support: NIH grant CA 001833-03 and National Health and Medical Research Council of Australia (Program no. 199600). D.C. Whiteman and N.K. Hayward are recipients of research fellowships from the National Health and Medical Research Council of Australia.

The costs of publication of this article were defrayed in part by the payment of page charges. This article must therefore be hereby marked *advertisement* in accordance with 18 U.S.C. Section 1734 solely to indicate this fact.

We thank the study participants and their families as well as the other Study of Digestive Health and Australian Cancer Study investigators for their contribution: Adele C. Green, Greg Falk, Peter G. Parsons, David M. Purdie, and Penelope M. Webb (Queensland Institute of Medical Research); Sandra J. Pavey (Princess Alexandra Hospital); and Glyn Jamieson (University of Adelaide).

The funding bodies played no role in the design or conduct of the study; the collection, management, analysis, or interpretation of the data; or the preparation, review, or approval of the manuscript.

References

1. Blot WJ, Devesa SS, Kneller RW, Fraumeni JF, Jr. Rising incidence of adenocarcinoma of the esophagus and gastric cardia. JAMA 1991;265:1287–9.
2. Blot WJ, McLaughlin JK. The changing epidemiology of esophageal cancer. Semin Oncol 1999;26:2–8.
3. Pohl H, Welch HG. The role of overdiagnosis and reclassification in the marked increase of esophageal adenocarcinoma incidence. J Natl Cancer Inst 2005;97: 142–6.
4. Hansen S, Wiig JN, Giercksky KE, Tretli S. Esophageal and gastric carcinoma in Norway 1958-1992: incidence time trend variability according to morphological subtypes and organ subsites. Int J Cancer 1997;71:340–4.
5. Vizcaino AP, Moreno V, Lambert R, Parkin DM. Time trends incidence of both major histologic types of esophageal carcinomas in selected countries, 1973-1995. Int J Cancer 2002;99:860–8.
6. Thomas RJ, Lade S, Giles GG, Thursfield V. Incidence trends in oesophageal and proximal gastric carcinoma in Victoria. Aust N Z J Surg 1996;66:271–5.
7. Lord RV, Law MG, Ward RL, Giles GG, Thomas RJ, Thursfield V. Rising incidence of oesophageal adenocarcinoma in men in Australia. J Gastroenterol Hepatol 1998;13:356–62.
8. Whiteman DC, Sadeghi S, Pandeya N, et al. Combined effects of obesity, acid reflux and smoking on the risk of adenocarcinomas of the oesophagus. Gut 2008;57:281–4.
9. Koppert LB, Wijnhoven BP, van Dekken H, Tilanus HW, Dinjens WN. The molecular biology of esophageal adenocarcinoma. J Surg Oncol 2005;92:169–90.
10. Galipeau PC, Prevo LJ, Sanchez CA, Longton GM, Reid BJ. Clonal expansion and loss of heterozygosity at chromosomes 9p and 17p in premalignant esophageal (Barrett's) tissue. J Natl Cancer Inst 1999;91:2087–95.
11. Riegman PH, Vissers KJ, Alers JC, et al. Genomic alterations in malignant transformation of Barrett's esophagus. Cancer Res 2001;61:3164–70.
12. van Dekken H, Geelen E, Dinjens WN, et al. Comparative genomic hybridization of cancer of the gastroesophageal junction: deletion of 14Q31-32.1 discriminates between esophageal (Barrett's) and gastric cardia adenocarcinomas. Cancer Res 1999;59:748–52.
13. Walch AK, Zitzelsberger HF, Bruch J, et al. Chromosomal imbalances in Barrett's adenocarcinoma and the metaplasia-dysplasia-carcinoma sequence. Am J Pathol 2000;156:555–66.
14. Calhoun ES, Gallmeier E, Cunningham SC, Eshleman JR, Hruban RH, Kern SE. Copy-number methods dramatically underestimate loss of heterozygosity in cancer. Genes Chromosomes Cancer 2006;45:1070–1.
15. Andersen CL, Wiuf C, Kruhoffer M, Korsgaard M, Laurberg S, Orntoft TF. Frequent occurrence of uniparental disomy in colorectal cancer. Carcinogenesis 2007;28:38–48.
16. Gaasenbeek M, Howarth K, Rowan AJ, et al. Combined array-comparative genomic hybridization and single-nucleotide polymorphism-loss of heterozygosity analysis reveals complex changes and multiple forms of chromosomal instability in colorectal cancers. Cancer Res 2006;66:3471–9.
17. Peiffer DA, Le JM, Steemers FJ, et al. High-resolution genomic profiling of chromosomal aberrations using Infinium whole-genome genotyping. Genome Res 2006; 16:1136–48.
18. Nancarrow DJ, Handoko HY, Stark MS, Whiteman DC, Hayward NK. SiDCoN: a tool to aid scoring of DNA copy number changes in SNP chip data. PLoS ONE 2007; 2:e1093.
19. Huang J, Gusnanto A, O'Sullivan K, Staaf J, Borg A, Pawitan Y. Robust smooth segmentation approach for array CGH data analysis. Bioinformatics 2007;23:2463–9.
20. Usener D, Schadendorf D, Koch J, Dubel S, Eichmuller S. cTAGE: a cutaneous T cell lymphoma associated antigen family with tumor-specific splicing. J Invest Dermatol 2003;121:198–206.
21. Hattrup CL, Gendler SJ. MUC1 alters oncogenic events and transcription in human breast cancer cells. Breast Cancer Res 2006;8:R37.
22. Burjonrappa SC, Reddimasu S, Nawaz Z, Gao X, Sharma P, Loggie B. Mucin expression profile in Barrett's, dysplasia, adenocarcinoma sequence in the esophagus. Indian J Cancer 2007;44:1–5.
23. Gleeson CM, Sloan JM, McGuigan JA, Ritchie AJ, Weber JL, Russell SE. Barrett's oesophagus: microsatellite analysis provides evidence to support the proposed metaplasia-dysplasia-carcinoma sequence. Genes Chromosomes Cancer 1998;21:49–60.
24. Michael D, Beer DG, Wilke CW, Miller DE, Glover TW. Frequent deletions of FHIT and FRA3B in Barrett's metaplasia and esophageal adenocarcinomas. Oncogene 1997;15:1653–9.
25. Hammoud ZT, Kaleem Z, Cooper JD, Sundaresan RS, Patterson GA, Goodfellow PJ. Allelotype analysis of esophageal adenocarcinomas: evidence for the involvement of sequences on the long arm of chromosome 4. Cancer Res 1996;56:4499–502.
26. Weiss MM, Kuipers EJ, Hermsen MA, et al. Barrett's adenocarcinomas resemble adenocarcinomas of the gastric cardia in terms of chromosomal copy number changes, but relate to squamous cell carcinomas of the distal oesophagus with respect to the presence of high-level amplifications. J Pathol 2003;199:157–65.
27. Arlt MF, Miller DE, Beer DG, Glover TW. Molecular characterization of FRAXB and comparative common fragile site instability in cancer cells. Genes Chromosomes Cancer 2002;33:82–92.
28. Arlt MF, Durkin SG, Ragland RL, Glover TW. Common fragile sites as targets for chromosome rearrangements. DNA Repair (Amst) 2006;5:1126–35.
29. Smith DI, McAvoy S, Zhu Y, Perez DS. Large common fragile site genes and cancer. Semin Cancer Biol 2007;17: 31–41.
30. Rumpel CA, Powell SM, Moskaluk CA. Mapping of genetic deletions on the long arm of chromosome 4 in human esophageal adenocarcinomas. Am J Pathol 1999; 154:1329–34.
31. Varis A, Puolakkainen P, Savolainen H, et al. DNA copy number profiling in esophageal Barrett adenocarcinoma: comparison with gastric adenocarcinoma and esophageal squamous cell carcinoma. Cancer Genet Cytogenet 2001;127:53–8.
32. Sterian A, Kan T, Berki AT, et al. Mutational and LOH analyses of the chromosome 4q region in esophageal adenocarcinoma. Oncology 2006;70:168–72.
33. Dolan K, Garde J, Walker SJ, Sutton R, Gosney J, Field JK. LOH at the sites of the DCC, APC, and TP53 tumor suppressor genes occurs in Barrett's metaplasia and dysplasia adjacent to adenocarcinoma of the esophagus. Hum Pathol 1999;30:1508–14.
34. Sanz-Ortega J, Hernandez S, Saez MC, et al. 3p21, 5q21, 9p21 and 17p13.1 allelic deletions are potential markers of individuals with a high risk of developing adenocarcinoma in Barrett's epithelium without dysplasia. Hepato-gastroenterology 2003;50:404–7.
35. Weir BA, Woo MS, Getz G, et al. Characterizing the cancer genome in lung adenocarcinoma. Nature 2007; 450:893–8.
36. Albrecht B, Hausmann M, Zitzelsberger H, et al. Array-based comparative genomic hybridization for the detection of DNA sequence copy number changes in Barrett's adenocarcinoma. J Pathol 2004;203:780–8.
37. Bian YS, Osterheld MC, Fontolliet C, Bosman FT, Benhattar J. p16 inactivation by methylation of the CDKN2A promoter occurs early during neoplastic progression in Barrett's esophagus. Gastroenterology 2002;122:1113–21.
38. Eads CA, Lord RV, Wickramasinghe K, et al. Epigenetic patterns in the progression of esophageal adenocarcinoma. Cancer Res 2001;61:3410–8.
39. Hardie LJ, Darnton SJ, Wallis YL, et al. p16 expression in Barrett's esophagus and esophageal adenocarcinoma: association with genetic and epigenetic alterations. Cancer Lett 2005;217:221–30.
40. Hall PA, Woodman AC, Campbell SJ, Shepherd NA. Expression of the p53 homologue p63α and ΔNp63α in the neoplastic sequence of Barrett's oesophagus: correlation with morphology and p53 protein. Gut 2001;49: 618–23.
41. Dunn J, Garde J, Dolan K, et al. Multiple target sites of allelic imbalance on chromosome 17 in Barrett's oesophageal cancer. Oncogene 1999;18:987–93.
42. Vijayakumar S, Garcia D, Hensel CH, et al. The human Y chromosome suppresses the tumorigenicity of PC-3, a human prostate cancer cell line, in athymic nude mice. Genes Chromosomes Cancer 2005;44:365–72.
43. Vissers KJ, Riegman PH, Alers JC, Tilanus HW, van Dekken H. Involvement of cancer-activating genes on chromosomes 7 and 8 in esophageal (Barrett's) and gastric cardia adenocarcinoma. Anticancer Res 2001;21: 3813–20.
44. Barrett MT, Galipeau PC, Sanchez CA, Emond MJ, Reid BJ. Determination of the frequency of loss of heterozygosity in esophageal adenocarcinoma by cell sorting, whole genome amplification and microsatellite polymorphisms. Oncogene 1996;12:1873–8.